JCI insight

Glucagon-like peptide-1 receptor agonism improves lung cancer outcomes and tumor growth control

Akhil Goud Pachimatla, Bailey Fitzgerald, Joyce Ogidigo, Meera Bhatia, Randall J. Smith Jr., Kalyan Ratnakaram, Sukumar Kalvapudi, Yeshwanth Vedire, Deschana Washington, Robert Vethanayagam rr, Hua-Hsin Hsiao, Spencer Rosario, Viraj R. Sanghvi, Joseph Barbi, Sai Yendamuri

JCI Insight. 2025. https://doi.org/10.1172/jci.insight.195484.

Clinical Research and Public Health | In-Press Preview | Clinical Research | Oncology

BACKGROUND. Emerging evidence indicates a reduced incidence of multiple cancers in users of Glucagon-like peptide-1 receptor agonists (GLP-1RAs), drugs widely used for glycemic control and weight reduction that modulate several key regulators of metabolism. We sought to examine their association with non-small cell lung cancer (NSCLC) outcomes in overweight and obese patients and gain mechanistic insights from mouse models.

METHODS. Two clinical cohorts of overweight and obese NSCLC patients—one undergoing surgical resection (n=1,177, 71 GLP-1RA users) and another receiving immune checkpoint inhibitors (ICIs; n=300, 10 GLP-1RA users), were propensity score matched for relevant covariates and analyzed for clinical outcomes.

RESULTS. GLP-1RA use was associated with increased recurrence-free survival in overweight and obese patients (HR=0.41 [95%CI=0.16-1.04], p=0.026) after lobectomy. GLP-1RA treatment reduced tumor burden in obese but not normal-weight mice and altered the frequency and phenotypes of leukocyte populations and gene expression patterns in obese tumors, crucial to cancer progression and anti-tumor immunity. Concurrent GLP-1RA and immunotherapy was associated with improved overall (0.41 [0.16-1.01], 0.027) and progression-free survival (HR=0.31, [0.10-0.94], 0.019) for patients with advanced NSCLC.

CONCLUSIONS. In our cohort, GLP-1RAs enhanced lung cancer-specific clinical outcomes and augment immunotherapy efficacy. Preclinical evidence suggested this effect to be obesity-restricted and mediated by immune modulation of the tumor microenvironment.

FUNDING. This work was supported by a generous donation from Mr. George Duke to […]

Glucagon-like peptide-1 receptor agonism improves lung cancer outcomes and tumor growth control

Akhil Goud Pachimatla[1]*, Bailey Fitzgerald[2] *, Joyce Ogidigo[3], Meera Bhatia[1], Randall J. Smith Jr.[4], Kalyan Ratnakaram[1], Sukumar Kalvapudi[1], Yeshwanth Vedire[1], Deschana Washington[4], Vethanayagam RR[1], Hua-Hsin Hsiao[5], Spencer Rosario[5], Viraj R. Sanghvi[3,6], Joseph Barbi[1,4#], Sai Yendamuri[1#]

*Both authors contributed equally to the study.

[1]Department of Thoracic Surgery, Roswell Park Comprehensive Cancer Center, Elm and Carlton Streets, Buffalo, NY, USA; [2]Department of Medical Oncology, Roswell Park Comprehensive Cancer Center, Buffalo, NY, USA; [3] Department of Medicine, Herbert Irving Comprehensive Cancer Center, Columbia University Irving Medical Center, New York, NY, USA; [4]Department of Immunology, Roswell Park Comprehensive Cancer Center, Elm and Carlton Streets, Buffalo, NY, USA; [5]Department of Biostatistics and Bioinformatics, Roswell Park Comprehensive Cancer Center, Buffalo, NY, USA; [6] Naomi Berrie Diabetes Research Center, Columbia University Irving Medical Center, New York, NY, USA.

[#]Co-corresponding authors:

Sai Yendamuri, MD, FACS, MBA,

Professor and Chair of the Department of Thoracic Surgery,

Roswell Park Comprehensive Cancer Center,

665 Elm St., Buffalo, NY. 14203

Phone: 716-364-4852

sai.yendamuri@roswellpark.org

Joseph Barbi, PhD,

Assistant Professor, Departments of Immunology and Thoracic Surgery,

Roswell Park Comprehensive Cancer Center,

665 Elm St., Buffalo, NY. 14203

Phone: 716-845-1189

joseph.barbi@roswellpark.org

Conflict of interest

None of the authors have any conflicts of interest.

Abstract:

Background: Emerging evidence indicates a reduced incidence of multiple cancers in users of Glucagon-like peptide-1 receptor agonists (GLP-1RAs), drugs widely used for glycemic control and weight reduction that modulate several key regulators of metabolism. We sought to examine their association with non-small cell lung cancer (NSCLC) outcomes in overweight and obese patients and gain mechanistic insights from mouse models.

Methods: Two clinical cohorts of overweight and obese patients with NSCLC—one undergoing surgical resection (n=1,177, 71 GLP-1RA users) and another receiving immune checkpoint inhibitors (ICIs; n=300, 10 GLP-1RA users), were propensity score matched for relevant covariates and analyzed for clinical outcomes.

Results: GLP-1RA use was associated with increased recurrence-free survival in overweight and obese patients (HR=0.41 [95%CI=0.16- 1.04], p=0.026) after lobectomy. GLP-1RA treatment reduced tumor burden in obese but not normal-weight mice and altered the frequency and phenotypes of leukocyte populations and gene expression patterns in obese tumors, crucial to cancer progression and anti-tumor immunity. Concurrent GLP-1RA and immunotherapy was also associated with improved overall (0.41 [0.16-1.01], 0.027) and progression-free survival (HR=0.31, [0.10-0.94], 0.019) for patients with advanced NSCLC.

Conclusions: In our cohort, GLP-1RAs enhanced lung cancer-specific clinical outcomes and augment immunotherapy efficacy. Preclinical evidence suggested this effect to be obesity-restricted and mediated by immune modulation of the tumor microenvironment.

Funding: This work was supported by a generous donation from Mr. George Duke to SY; W81XWH-21-1-0377, (GM147497), and RSG-22-071-01-TBE to VRS; 1R01 CA255515-01A1 to SY and JB; and NIH/NCI Cancer Center Support Grants P30CA013696 and P30CA016056.

Keywords: Obesity, GLP-1 Receptor Agonists, Lung Cancer, NSCLC

Introduction:

Glucagon-like peptide-1 Receptor Agonists (GLP-1RAs), initially introduced as a class of anti-diabetic drugs, have entered widespread use after their recent approval for the treatment of obesity and obesity-related conditions (1). Several retrospective studies further associate GLP-1RA use with altered cancer incidence, yet the underlying mechanisms remain unclear (2, 3).

Although the relationship between obesity and lung cancer risk is contentious, with some studies reporting a paradoxically reduced risk of lung cancer in obese populations (the so-called ‘obesity paradox'), evidence generated by our group and others now supports a correlation between excess visceral fat and obesity-related lung cancer risk (4, 5).

Visceral adiposity induces multiple changes in metabolic pathways, resulting in chronic meta-inflammation and suppression of anti-tumor immunity. Specifically, it is known to hamper the function of CD8+ T cells (6), key mediators of the immune response against cancer, while broadly upregulating the expression of inhibitory immune checkpoint molecules such as programmed cell death protein 1 (PD-1) (7) and enhancing suppressive leukocyte populations (8). Previous studies demonstrate that metformin, another common anti-diabetic agent, can reverse multiple obesity-associated immune disturbances and improve lung cancer outcomes in overweight and obese individuals (9). Given that GLP-1RAs are effective in promoting weight loss and reducing visceral adiposity (10), we hypothesized that GLP-1RAs may similarly counteract the detrimental effects of obesity on anti-tumor immunity and disease progression, leading to improved non-small cell lung cancer (NSCLC) outcomes.

To test our hypothesis, we first interrogated the in vitro effects of the GLP-1RA liraglutide on murine lung cancer cell lines. We then examined the effects of distinct GLP-1RA drugs on tumor

growth dynamics in vivo using both implantable and KRAS-mutated, autochthonous murine lung cancer models, scrutinizing the effects of GLP-1RA treatment on the immune tumor microenvironment (TME). Finally, in an exploratory analysis, we performed two retrospective analyses of real-world single center outcomes data for patients with NSCLC treated with GLP-1RA, first in a post-surgical setting, and then in advanced disease in combination with immune checkpoint inhibitors (ICI).

Results:

Liraglutide does not impair murine lung cancer cell proliferation in vitro

We investigated the *in vitro* effect of liraglutide on KPN 1.1 (Kraslox-stop-lox(lsl)-G12D/+; p53flox/flox- NINJA) and Lewis Lung Carcinoma (LLC) cell proliferation. Based on reported steady-state plasma concentrations of liraglutide ranging from 20-40 nM for typical clinical doses (0.6-1.8 mg), we examined a range of concentrations: 0, 10, 30, 90, 270, and 810 nM. Cell proliferation was assessed by measuring the fold change in absorption values after 48 hours of treatment. There was no significant difference in cell proliferation for KPN1.1 cells across liraglutide concentrations, while LLC cells exhibited increased proliferation at higher drug concentrations (Supplemental Figure 1, A, B).

Liraglutide inhibits the progression of implanted tumor growth in obese, but not normal weight mice.

We next investigated the effect of liraglutide on tumor growth in vivo. Here, normal weight (lean) C57BL/6 mice and those with diet-induced obesity (DIO) were challenged with subcutaneous (s.c.) injection of KPN1.1 lung cancer cells. Upon detection of palpable s.c.

tumors, mice received daily liraglutide (0.2 μg/g body weight) or a PBS vehicle intraperitoneally. While liraglutide-treated mice exhibited a slight decrease in body weight during the experiment, and control mice showed an increase (weight change: -0.78 g vs. +0.98 g, respectively; (Supplemental Figure 2. A, B), no statistically significant difference was observed in mean tumor volumes or final tumor weight (0.98 g vs. 1.04 g; $p = 0.67$) in normal weight/lean mice (Figure 1. A, B). In contrast, liraglutide administration significantly inhibited the progression of tumor growth, as evidenced by reductions in tumor volumes and weight (1.07 g vs. 1.86 g; $p = 0.03$) relative to the vehicle group (Figure 1. C, D). Of note, liraglutide-treated DIO mice demonstrated greater weight reduction compared to their respective controls (13.46 g vs. 4.06 g, respectively; Supplemental Figure 2. A, B).

RNA sequencing reveals GLP1-RA altered pro-tumor gene expression in mice with implanted lung cancers.

To gain insight into the mechanism underlying the benefits of GLP-1RA suggested by clinical and preclinical studies, tumor gene expression was compared in liraglutide- and vehicle-treated s.c. tumors harvested in DIO mouse model studies using RNA Sequencing (RNASeq). Of the 35,141 transcripts assessed, 27 were differentially expressed significantly (adjusted p-value < 0.05 and $|\log FC| > 0.58$, Figure 2A). The transcripts upregulated with liraglutide treatment (Figure 2A, green) included *Igfbp7*, which induces G1 phase cell cycle arrest by upregulating cyclin-dependent kinase inhibitors. Additionally, treatment was associated with increased *Creb3l1*, a regulator of angiogenesis (11), and *Nfix*, which encodes a factor with pro- and anti-tumor roles that are also involved with immune cell development and differentiation (12). Conversely, liraglutide exposure was also associated with decreased *Anxa10*, a well-known

marker of poor prognosis with a role in various cell-signaling pathways (13). Further, the drug was linked to reduced expression of the pro-tumor genes *Higd1a* and *Rpl39*, associated with hypoxia cellular stress and metabolism, and cell proliferation and migration, respectively (14, 15).

Gene set enrichment analysis (GSEA) revealed significant treatment effects on several pathways relevant to cancer outcomes (normalized enrichment score > 2, q-value < 0.05) spanning cell proliferation, cellular respiration, immune signaling, and cell signaling (Figure 2B). Notably, genes linked to signaling triggered by interferon-gamma (an anti-tumor immunity-promoting cytokine) and growth factor (Insulin-derived growth factor) signaling were significantly upregulated with liraglutide treatment. Several metabolic pathways important for tumor and leukocyte biology, including fatty acid (sphingolipids) and amino acid metabolism, were enhanced and disrupted, respectively, and genes important for translation-associated processes were also apparently suppressed with treatment, as were those associated with poor lung cancer survival. Finally, multiple cell signaling pathways well appreciated for driving tumor development and progression were also suppressed in GLP-1RA treated tumors, including those involving *KRAS*, *EGFR*, *MYC*, and *E2F* transcription factors (Figure 2B). Overall, these findings link liraglutide with gene expression changes in the tumor relevant to immunity, metabolism, and tumor progression that are likely to reflect or explain the effects of GLP-1RA seen in mice and patients.

GLP-1RA treatment enhances anti-tumor immune responses in mice.

The GLP-1R is expressed in several leukocyte populations (16), but the effects of GLP-1RA on these cells are apparently complex, and their likely impact on the anti-tumor immune response is unclear. While many have found the effects of GPL-1R signaling and agonism to be immune-suppressive (17), some studies suggested enhanced anti-tumor immunity (18, 19). To explore whether liraglutide's anti-tumor effects in our mouse model studies stem from favorable modulation of anti-tumor immunity, we used flow cytometry to characterize the phenotypic and functional changes among the tumor-infiltrating leukocytes (TILs) associated with treatment in harvested s.c. tumors.

Increased CD4+ T cell and Natural-killer (NK) cell frequencies in the tumors of GLP-1RA-treated obese mice were seen (Figure 3A, B). Proportions of conventional (i.e., non-regulatory) CD4+ T cells (Tcon), marked by the activation marker CD69, were also elevated in liraglutide-treated mice (Figure 3C)–potentially indicating an enhanced anti-tumor immune response. Interestingly, the fraction of intratumor CD8+ and Tcon compartments with an effector surface marker profile ($CD44^{high}/CD62L^{low}$) was apparently reduced in favor of CD44+/CD62L+ T cells (Figure 3D, E), suggesting a potential shift towards a memory-like phenotype in these cells.

Since Foxp3+ Regulatory T cells (Tregs) express relatively high levels of the GLP-1 receptor (20), and a role for its downstream signaling has been reported to maintain these suppressor cells in the periphery (21), we assessed liraglutide-triggered changes among tumor Tregs. Surprisingly, proportions of Foxp3+/CD25+ cells within the TIL CD4+ pool were significantly reduced with treatment (Figure 3F). Interestingly, the functionally potent, activated (CD44+/CD62L-) or "eTreg" subpopulation made up a smaller portion of the TIL-Treg pool from liraglutide-treated mice compared to vehicle-treated control mice, in favor of a population

with memory-like potential (i.e., CD44+/CD62L+ surface staining) (Figure 5G). In agreement with a prior study (20), GLP-1RA treatment upregulated PD-1 and PD-L1 on tumor Tregs (Supplemental Figure 3A, B), however increased levels of mTOR activity (indicated by phosphorylated mTOR (p-mTOR)+/Foxp3+ T cells) and Tbet expression were found among GLP-1RA-treated Tregs as well (Supplementary Figure 3C, D). This combination indicates an activated but unstable Treg phenotype (22-25), less capable of restricting robust anti-tumor immune response suppression. Collectively, these results suggest the ability of GLP-1RA to undermine immune suppression in obese mice.

Additional effects of GLP-1RA treatment were evident in antigen-presenting cell (APC) populations in the tumor niche. Dendritic cells (DCs) and macrophages from treated mice displayed upregulated MHC II levels, an effect that approached and achieved statistical significance in these populations, respectively (Figure 3H). Conversely, TILs of the GLP-1RA harbored markedly fewer APCs producing indoleamine 2,3-dioxygenase (IDO) (Figure 3I), a mediator of tumor-associated immune suppression and a mechanism of Treg expansion and differentiation (26, 27). The mice treated with liraglutide also displayed a relative scarcity of arginase-expressing myeloid-derived suppressor cells (MDSCs) (Figure 5J). Thus, it is possible that GLP-1RA triggers APC phenotypes poised to effectively stimulate T cell responses and cell-mediated anti-tumor immunity. Further supporting this notion, the pool of TIL-isolated CD4+ T cells recovered from liraglutide-treated mice capable of producing pro-inflammatory, tumoricidal cytokines ex vivo was expanded (Figure 3K). In all, these findings support a potent immunostimulatory effect of the GLP-1RA liraglutide impacting several leukocyte populations that may be responsible for the improved tumor growth control and clinical outcomes linked to the drug.

Semaglutide inhibits tumor progression and improves survival in a KRAS-driven mouse lung cancer model.

To reduce the impact of model-specific or drug-specific factors on tumor dynamics, we repeated our experiment examining the effects of GLP-1RA administration on murine tumor growth, this time in an independent autochthonous mouse model with conditional *KrasG12D* activation and *Trp53* deletion (KP) using the GLP-1RA semaglutide. To induce obesity, tumor-free KP mice were pre-fed a high-fat Western diet (WD; 60% kcal from fat) supplemented with sugar water (23.1 g/L D-fructose and 18.9 g/L D-glucose) for 13 weeks prior to tumor initiation (Fig. 4A). Lung adenocarcinoma was initiated via intratracheal delivery of Cre recombinase; this precipitates spontaneous tumor growth which more closely mimics the geographic pattern of human lung cancer metastases compared to subcutaneous implantation. The KP mice with DIO and induced lung adenocarcinoma were treated with semaglutide (N=7) or vehicle control (N=7).

Semaglutide treatment significantly extended overall survival (HR: 0.21, 95% CI: 0.057–0.79, p = 0.012) compared to vehicle-treated control (Fig. 4B). Longitudinal μCT revealed significantly reduced tumor burden in the semaglutide groups (Fig. 4C), mirroring the results of our heterotopic models, where GLP-RA reduced tumor growth and progression in obesity-associated lung cancer**.**

GLP-1RA use is associated with improved Recurrence Free Survival (RFS) after NSCLC resection

We then performed a retrospective examination of clinical outcomes in a database of patients undergoing surgery for NSCLC at our center between 2015 and 2024. A total of 1,177 patients met criteria for inclusion in the post-surgical cohort (a flowchart of the cohort is represented in supplemental figure 4A). Within this cohort, 71 patients were GLP-RA users. Demographic characteristics, including age, clinical stage, race, and smoking history were generally well balanced between the GLP-1RA users and non-users, however GLP-1RA users had significantly higher mean Body Mass Index (BMI) at the time of resection than the non-users (35.07 vs 30.6; p = 0.001). Demographic data are reported in supplementary table 1. Most patients across both groups had clinical-stage I disease 970 (82.4%), while 193 (16.4%) had stage II, and 14 (1.2%) had stage III lung cancers.

In an unmatched, univariate cox-regression model including the entire cohort, GLP-1RA use was associated with improved RFS (HR: 0.41; 95% CI: 0.17- 1.02; p = 0.027). No such association was noted for OS (HR: 0.70; 95% CI: 0.43- 1.16; p = 0.09).

In a propensity matched analysis, where propensity scores were calculated using age, sex, race, BMI, cancer stage, smoking status, and histology as covariates and GLP-1RA use as the dependent variable, a matched cohort of 629 was identified which included 560 GLP-1RA non-users and 69 GLP-1RA users. This cohort did not include any patients with stage III disease (see supplemental table 1). Univariate Cox regression of matched cohort showed that GLP-1RA use was associated with improved RFS (HR = 0.41, 95% CI: 0.16–1.04, p = 0.026; Figure 5A). GLP-1RA use was not significantly associated with OS (HR = 0.78, 95% CI: 0.44–1.38, p = 0.20;

Figure 5B). Results of univariate analyses for all the covariates in both unmatched and matched cohorts are presented in Table 1.

GLP-1RA use improved survival in overweight patients receiving immune checkpoint inhibitors (ICI) for advanced NSCLC.

In light of the findings from the preclinical model and expanding use of immunotherapy in the treatment of lung cancer, we set out to test whether the apparent benefits of GLP1-RA use extend to patients on ICI therapy. A cohort of 300 patients with advanced lung cancer treated with ICI at our center between 2015 and 2023 was identified, of which 10 patients were prescribed concurrent GLP-1RA. A flowchart of the cohort is represented in supplemental figure 4B. All GLP-1RA users in the cohort had diabetes (reflecting FDA approved indications during our study period), whereas 25% of non-users were diabetic. Most patients (78.7%) had stage IV disease; the remainder of the cohort was comprised of stage III NSCLC not amenable to local treatments. Treatment included immunotherapy alone for 158 patients (52.7%) and a combination of immuno- and chemotherapy for 142 (47.3%). Patients receiving GLP-1RA were significantly younger; other characteristics such as gender, BMI, race, smoking status, tumor histology, and treatment modality were similar between groups (Supplemental Table 2).

In an unmatched analysis, univariate cox-regression modeling demonstrated that GLP-1RA use was associated with improved PFS (HR: 0.39; 95% CI: 0.13- 1.14; p = 0.044) and OS (HR: 0.40; 95% CI: 0.15- 1.04; p = 0.031).

In a propensity matched analysis, propensity scores were calculated using age, sex, race, smoking status, BMI, tumor histology, first-line therapy, stage at the start of ICI therapy, as covariates with GLP-1RA use as the dependent variable. The matched cohort (n=89) had 79 non-

users and 10 GLP-1RA users (see supplemental table 2). Univariate Cox regression of the matched cohort showed that GLP-1RA use was associated with improved PFS (HR = 0.31, 95% CI: 0.1–0.94, p = 0.019; Figure 6A) and OS (HR = 0.41, 95% CI: 0.16–1.01, p = 0.027; Figure 6B). Results of univariate analyses for all covariates in both unmatched and matched cohorts are presented in Table 2.

Discussion:

The use of GLP-1RA in the United States is rising dramatically, with expanding indications for both diabetes and obesity-related conditions (28, 29). Since these conditions also affect the majority of patients diagnosed with lung cancers (30), widespread use of these medications during treatment for lung malignancies is inevitable. Little is known about the safety of GLP-1RA use during lung cancer treatment, however, and any impact these medications may have on treatment outcomes is similarly opaque. While the effects of GLP-1RA on the incidence of liver, pancreatic, colorectal, genitourinary, cutaneous, and hematologic malignancies have been reported (29) the present study marks the first attempt to examine the drug family's impact on lung cancer outcomes and the potential utility of GLP-1RA with ICI.

Unsurprisingly given our hypothesized mechanism of action, we observed little effect of GLP-1RA on in vitro cell proliferation. These findings are in line with previous studies in the preclinical arena involving multiple cancer types which have reported inconsistent direct effects of GLP-1RA on cancer cell proliferation (31-35), and they suggest that substantial inhibitory effects on malignant cells are unlikely. Notably, however, we observed consistent and significantly reduced tumor burden in both implanted and autochthonous mouse lung cancer models treated with GLP-1RA. Thus, we suspect that the reduction in tumor growth seen in obese mice treated with GLP1-RA may be linked to biological pathways active within the TME.

Indeed, our preclinical mouse studies provide some mechanistic insights in support of this notion. Parallel transcriptomic analysis substantiated an immune-stimulating effect of GLP-1RA, revealing marked treatment-associated alterations in pathways related to oncogenesis, tumor cell proliferation, and metabolism, which may modulate complex biological processes intrinsic as well as extrinsic to malignant cells themselves. Our subcutaneous tumor model showed that

liraglutide, a widely used GLP-1RA, inhibited tumor growth selectively in obese mice and also revealed multifaceted immune-related changes in the tumor microenvironment consistent with enhanced anti-tumor immunity. These included increased CD4+ T cell and NK cell frequencies, bolstered pools of memory-like T cells, reduced Treg populations, and apparent improvements in APC functionality. Interestingly, changes in gene expression profiles closely resembled those observed in individuals with elevated total fat areas (36). That study, which examined genomic alterations in NSCLC patients with high versus low body fat, revealed similar changes in transcripts associated with cell proliferation, signaling, and apoptosis, apart from genes regulating fatty acid metabolism. These findings indicate that liraglutide may exert its effects by modulating cellular pathways in a manner that counteracts obesity-induced metabolic adaptations, potentially leading to improved clinical outcomes.

The immunological effects we observed are notable in that they run surprisingly counter to much of the existing literature speaking to the immunomodulatory properties of GLP-1 and GLP-1RA, which generally support a role in immune suppression in various settings. For example, GLP-1 has been convincingly characterized as a mediator of negative costimulation in T cells, with agonism leading to *suppression* of proliferation and allograft rejection in mouse studies. In contrast, GLP-1R antagonism, via exe9 bolstered anti-tumor immunity when tested in a colorectal cancer model (37). Additional studies have characterized the activity of GLP-1RA drugs as anti-inflammatory (38), and reports have suggested both high expression of the GLP-1 receptor by Treg cells (20) and a role for GLP-1 signaling in the biology of these suppressive cells (21, 39). On the other hand, our findings do resonate with a recent preclinical study that found the GLP-1RA semaglutide slows tumor growth and spread, enhances T cell responses and dendritic cell maturation, and undermines Tregs while showing no direct effects on breast cancer

cell lines in vitro (19). Other studies have also suggested anti-tumor promise for liraglutide in a model of hepatocellular carcinoma, where it can activate NK cell-mediated responses (40). Others have found the drug can improve the anti-tumor effects of ICI by down-modulating additional regulators of inflammation in mouse tumor models (41, 42).

Moreover, our retrospective clinical studies provide early evidence that this effect may translate into human NSCLC. We found that in early-stage NSCLC patients undergoing surgery at our institution, GLP-1RA in the postoperative period improved RFS. Following the animal experiments and in vitro assays, analysis of GLP-1RA use in advanced-stage NSCLC patients receiving ICI demonstrated augmented benefit, with improvement in both PFS and OS. While these results are preliminary, they are suggestive and support further investigation into this drug family as a means to improve lung cancer treatment outcomes in obese patients with NSCLC.

There are several important limitations in our study which provide opportunities for future investigations. Our preclinical studies were conducted with semaglutide and liraglutide, as these drugs were the most common in clinical use prior to 2024. These drugs are both single GLP-1RA medications without co-agonism of Gastric Inhibitory Polypeptide (GIP) and follow up studies are needed to confirm that our results are conserved across newer dual agonist drugs, such as tirzepatide. Additionally, while our analysis of the transcriptomic and immunological impact of GLP-1RA treatment in obese tumors reveal previously uncharted effects, a definitive mechanism remains to be elucidated. It is also unclear whether the immunological changes and anti-tumor effects we observe stem from a direct action of the drug on leukocytes (a distinct possibility since many immune cells have been shown to express the GLP-1 receptor) or indirect effects arising from a correction of excess adiposity – a state known to oppose effective anti-tumor responses. However, given the incremental (albeit statistically significant) correction in obesity

seen and the fact that obese mice (43) and cancer patients (44) often respond better to ICI therapy than normal weight counterparts in the absence of weight loss, the latter possibility seems less likely to explain the benefits of GLP-1RA in our study.

We are also cautious to avoid over interpretation of our clinical analysis, which is inherently limited by its retrospective nature and small, single center sample size. To address this weakness and mitigate the effects of confounders in the design, we supplemented our unmatched univariate analysis with propensity score matched analysis, however the small numbers make multivariate analysis impossible without substantial risk of introducing type I error, so contribution of effects such as degree of weight loss and other baseline characteristics cannot be delineated. In every case the need for prescription GLP-1RA was determined by non-oncology treating physicians, which may introduce selection bias. Moreover, all patients within this cohort were prescribed GLP-1RA for diabetes, as this was the only FDA-approved indication during the study period. Nevertheless, as the indications for GLP1-RA treatment expand and databases including larger numbers of patients become available, further work investigating outcomes in larger populations will be worthwhile. Collectively, these limitations and lingering questions highlight the need to better understand the action GLP-1RA modulators of metabolism and NSCLC. Such knowledge gaps provide rationale for pilot clinical trials where safety can be confirmed, and more correlative translational work can be done to compare the effects seen in our preclinical models to those in the human NSCLC TME.

While these and additional mechanistic studies are needed to fully realize the implications of our findings for future NSCLC therapy, this study provides encouraging, albeit preliminary, evidence regarding the favorable effects of GLP-1RA use after resection and during ICI treatment for NSCLC. In the context of rising obesity rates and high global lung cancer mortality, these

observations may be important for adapting the treatment of lung cancer to a changing patient pool, and they warrant further investigation in the direction of mitigating obesity-associated lung cancer risk.

Materials and Methods:

Sex as a biological variable

Male mice were used in these lung cancer preclinical models to facilitate creation of DIO models as male C57BL/6 mice more uniformly display significant weight gain on high fat diets (relative to normal diet controls) than females(45-47). This approach is consistent with established protocols in the field and facilitates direct comparison with previous studies.

In vitro effects of liraglutide on murine lung cancer cell lines

The murine lung cancer cell lines KPN 1.1 (48) (provided by Dr. N. Joshi, Yale School of Medicine, New Haven, CT) and Lewis Lung Carcinoma (LLC; ATCC # CRL-1642-LUC2) were cultured in vitro and harvested in the logarithmic phase by trypsinization, followed by centrifugation. Cell concentration was adjusted and added to strip-well plates at 3000 cells per well, which were then incubated at 37°C. After 24 hours, the cells were treated with liraglutide at 10, 30, 90, 270, and 810 nM concentrations. To measure the cell proliferation rate, the wells were washed, and 95 μL of cell culture medium and 5 μL of CCK-8 reagent (Dojindo Laboratories) were added to each well. The strips were allowed to incubate at 37 °C for 2 h, and the absorbance value (OD value) was measured and recorded using a microplate reader at a wavelength of 450 nm at 0, 24, 48, 72, and 96 hr. The cell proliferation rate was calculated as follows: cell proliferation rate = (OD value at a given concentration at 48-hour timepoint-blank)/ (OD value on day 0-blank).

Effects of GLP1-RA on murine survival, subcutaneous tumor dynamics, gene expression and tumor immune microenvironment in an implanted lung cancer model.

Age-matched obese and non-obese male C57BL/6 mice were purchased (The Jackson Laboratory, ME, US; strain numbers 380050, 380056) or generated in-house by feeding normal weight mice with high fat (60% calories from fat, 5.4 kCal/g) or control chow (~7.2% calories from fat, 3.9 kCal/g) (Bio-Serv, NJ, USA, products #S3282 and #F4031, respectively). For s.c. tumor challenge experiments, KPN 1.1 cells or LLC cells were injected into the flanks of 7–17-week-old obese and non-obese mice (75,000 cells per mouse). Mice with palpable tumors (typically detected 6-7 days post-implantation) received intraperitoneal injections of liraglutide (0.2 ug per gram of mouse body weight) or Phosphate-buffered saline (PBS) vehicle daily. The mice were euthanized after 19-22 days of cell inoculation, and tissues were harvested for further analysis.

RNA sequencing was performed on excised, subcutaneous KPN1.1 tumors from obese mice treated with GLP-1RA. At the time of mouse tumor harvest, a fragment was flash frozen and was later used for RNA isolation using the miRNeasy mini kit (Qiagen). The sequencing libraries were prepared with the RNA HyperPrep Kit with RiboErase (HMR) kit (Roche Sequencing Solutions), from 500ng total RNA. Following the manufacturer's instructions, the first step depletes rRNA from total RNA. After ribosomal depletion, the remaining RNA is DNase-digested to remove any gDNA contamination. Samples are then purified, fragmented, and primed for cDNA synthesis. Fragmented RNA is then reverse-transcribed into first-strand cDNA using random primers. The next step removes the RNA template and synthesizes a replacement strand, incorporating dUTP in place of dTTP to generate ds cDNA. Pure Beads (KAPA BIOSYSTEMS)

are used to separate the ds cDNA from the second-strand reaction mix, resulting in blunt-ended cDNA. A single 'A' nucleotide is then added to the 3' ends of the blunt fragments. Multiple indexing adapters, containing a single 'T' nucleotide on the 3' end of the adapter, are ligated to the ends of the ds cDNA, preparing them for hybridization onto a flow cell. Adapter-ligated libraries are amplified by PCR, purified using Pure Beads, and validated for appropriate size on a 4200 TapeStation D1000 Screentape (Agilent Technologies, Inc.). The DNA libraries are quantified using KAPA Biosystems qPCR kit, and are pooled together in an equimolar fashion, following experimental design criteria. Each pool is denatured and diluted to 350pM with 1% PhiX control library added. The resulting pool is then loaded into the appropriate NovaSeq Reagent cartridge for 100 paired-end sequencing and sequenced on a NovaSeq6000 following the manufacturer's recommended protocol (Illumina Inc.). Raw reads that passed the Illumina RTA quality filter were demultiplexed and pre-processed using FastQC for sequencing base quality control. Reads were then mapped to the latest version of a mouse reference (GRCm39/mm39) using Bowtie (v1.0.1) (49) and TopHat (v2.0.13) aligner (50). Mapped reads were quantified at the gene level as a raw counts matrix using featureCounts from Subread (51). Samples were filtered after quality assessment, and a total of 10 samples were used in subsequent analyses (n=5/group). Raw feature counts were normalized, and differential expression analysis was carried out using DESeq2 (52), and visualized using volcano plots. Differential expression rank order was used for subsequent gene set enrichment analysis (GSEA) (53), performed using the cluster profile package in R, and visualized via lollipop plots. Gene sets queried included the Hallmark, Canonical pathways, and GO Biological Processes Ontology collections available through the Molecular Signatures Database (MSigDB) (54).

Flow cytometry analysis was performed on the s.c. KPN1.1 tumors excised from obese mice treated with GLP-1RA. Tumors were cleaned of skin and fat before mechanical (GentleMACS dissociation) and enzymatic digestion in a collagenase/hyaluronidase mix (Stem Cell Technologies) following the manufacturer's protocol. The resulting cell suspensions were filtered (100 μm cell strainer), washed, and pelleted before RBC lysis in 1 mL ACK buffer (Thermo Fisher Scientific). Cells were then washed with PBS containing 1% Fetal Bovine Serum (FBS) and 2mM EDTA before incubation with fluorochrome-conjugated antibodies diluted in like buffer. After surface immunostaining, intracellular markers (i.e., FOXP3) were stained after fixation and permeabilized using eBioscience's FOXP3 staining kit. For intracellular cytokine staining, cell suspensions were re-stimulated in media containing PMA and Ionomycin in the presence of Golgi-Plug (BD) for 5 hours at 37 °C before surface staining, fixation/permeabilization, and internal staining with anti-IFNγ and TNFα antibodies. Samples were run on an Aurora spectral flow cytometer (Cytek) before data analysis via OMIQ.

Effect of semaglutide on survival in an autochthonous KRAS-driven murine lung cancer model

$Kras^{LSL\text{-}G12D}$; $Trp53^{fl/fl}$ (KP) mice (*55*) (Jackson Laboratory #032435) were fed a high-fat Western diet (WD; 60% kcal fat, Research Diets #D12492) with sugar water (23.1 g/L D-fructose + 18.9 g/L D-glucose) ad libitum for 13 weeks to induce diet-induced obesity (DIO). Lung tumors were initiated via intratracheal adenoviral Cre recombinase (Ad-Cre; 2.5×10^7 PFU; University of Iowa Viral Core) (56-59).Tumor-bearing DIO-KP mice were randomized to receive intraperitoneal semaglutide (60 nmol/kg/ 0.25 μg/gm body weight, 3×/week; Cat #S9697; Selleck Chemicals, Houston, TX, USA) or saline (pH 7.4; Cytiva, Marlborough, MA, USA) (60). Imaging was conducted through the Oncology Precision Therapeutics and Imaging Core (OPTIC Core) at the

Columbia University Herbert Irving Comprehensive Cancer Center. High-resolution microcomputed tomography (μCT) was performed to assess lung tumor burden, as previously described (61).

Effects of GLP1-RA on survival outcomes in two retrospective clinical cohorts

Two distinct single-center clinical cohorts were manually curated and analyzed.

In a post-surgical cohort, medical charts for patients undergoing surgical resection at Roswell Park Cancer Institute (RPCI) between 2015-2024 were manually curated. Patients were included for analysis if they had (a) histologically confirmed non-small cell lung cancer (NSCLC) (b) BMI >25. Patients were defined as GLP-1RA users if they had GLP-1RA prescribed for >6 months during the period between resection and any event (defined as disease recurrence, death, or loss to follow up).

In an advanced disease cohort, medical charts for patients undergoing treatment for advanced or metastatic lung cancer at Roswell Park Cancer Institute (RPCI) between 2015-2023 were manually curated. Patients were included for analysis if they had: (a) histologically confirmed advanced or metastatic NSCLC, (b) received at least 3 doses of an anti-PD-(L)1 and/or anti-CTLA-4 immune checkpoint inhibitor (c), received no definitive local therapy (surgery or radiotherapy) and (d) had a BMI >25. Patients were again defined as GLP-1RA users if they had GLP-1RA prescribed for >6 months during the period between the start of ICI treatment and any event (defined as disease progression, death, or loss to follow up).

In both cohorts, patient demographics, including age, sex (male or female), race (white and non-white), smoking status (current, former, never smokers), and BMI were collected.

Visceral Fat Indexes and abdominal circumference were not routinely available in this retrospective database. For the surgical cohort, recurrence free survival (RFS) was calculated from the date of resection until disease recurrence, death, or censoring at loss to follow up. For the advanced disease cohort, progression free survival (PFS) was used, calculated from the date of treatment initiation until disease progression, death, or censoring at loss to follow up. Overall survival (OS) was defined from the point of resection in the post-surgical cohort and start of treatment in the advanced disease cohort until the date of death or censoring at loss to follow up.

Statistical methods

In the retrospective cohort analysis, results are reported as RFS, PFS, and OS as appropriate to the clinical scenario. To reduce confounding from baseline differences in small sample sizes, propensity scores were initially estimated using logistic regression with GLP-1RA use as the dependent variable. Propensity score matching was subsequently performed using greedy nearest-neighbor matching with a fixed control-to-treated ratio of 10:1 and a caliper width of 0.2 on the propensity score. The matching procedure was implemented in SAS version. 9.4 using PROC PSMATCH. Survival analysis was done using Cox proportional hazards regression on the matched cohort, accounting for the matched sets through stratification or clustering. Group differences were assessed using independent t-tests and chi-square tests. All statistical tests are 2-sided with a level of significance of 5%. OS and PFS analyses were conducted using Cox proportional hazards modeling for univariate models. The statistics for survival analysis are expressed in terms of hazard ratio, and 95% confidence interval with a one-sided p-value at a 5% level of significance. For animal model studies and in vitro experiments, the group differences were calculated using t-tests or 2-way ANOVA tests. Statistical analyses were performed using SPSS version 28.0.1.0 or GraphPad Prism version 9. Flow cytometry analysis was performed using OMIQ.

Study approval

The retrospective study protocol was reviewed and approved by the Institutional Review Board of Roswell Park Comprehensive Cancer Center (BDR 115119), and individual patient consents were waived. All animal experiments conducted were reviewed and approved by the Institutional Animal Care and Use Committee (IACUC) of Roswell Park Comprehensive Cancer (Protocols 1487 and 1349) or by Columbia University IACUC guidelines (Protocol AABV8661).

Data availability

Roswell Park Comprehensive Cancer IRB protocols prohibit the sharing of clinical data to protect patient privacy. The data from mice experiments is available as an .XLS file titled "Supporting data values". Flow cytometry data will be made available as raw data files upon request. Gene sequencing data have been deposited in the National Center for Biotechnology Information Gene Expression Omnibus (NCBI GEO) under accession number GSE302656.

Author contributions

SY, BF, JB, and VRS contributed to the conceptualization of the study. SY and BF supervised the clinical aspects, while JB and VRS guided the translational components. AP, SK, and YRV curated the clinical data. AP performed formal analysis of the clinical cohorts. AP, MB, KR, and VRR carried out animal experiments. RJS and DS conducted and analyzed flow cytometry experiments. HH and SR performed and supervised RNA sequencing analyses. JO and VRS contributed data and results from the autochthonous model. AP, BF, and JB wrote the original draft, with data visualization by AP, RJS, and SR. All authors reviewed and approved the final manuscript.

Both AP and BF are designated as co–first authors, as each contributed to equally critical aspects of the manuscript-AP led most of the analysis, conducted the mouse experiments, and prepared the initial draft, while BF was primarily responsible for conceptualization and revision of the manuscript. AP is listed first due to academic junior status and alphabetical order.

Submission declaration:

A part of this study was submitted and presented at the Academic Surgical Congress – Annual Meeting 2025. This manuscript or any part of it is not under consideration for publication elsewhere.

Acknowledgments

This work was supported by a generous donation from Mr. George Duke to SY via an institutional donor-advised fund in the Department of Thoracic Surgery. The funders had no role in study design, data collection and analysis, decision to publish, or preparation of the manuscript. DW is a CLIMB/IMSD Scholar supported by a grant from the National Institute for General Medical Sciences to the State University of New York at Buffalo. JB and SR are TREC Training Workshop Fellows (R25CA203650). The authors thank the staff of these shared resources at the Roswell Park Comprehensive Cancer Center for helpful discussion and assistance: Flow Cytometry and Imaging, Genomics and Translational Imaging, and Comparative Oncology. SY and JB are supported by 1R01 CA255515-01A1. VRS is supported by a Career Development Award from the Department of Defense (W81XWH-21-1-0377), R35/MIRA from NIH/NIGMS R35 (GM147497), and Research Scholar Grant from the American Cancer Society (RSG-22-071-01-TBE). JOO is partially supported by a Trainee Award from the Herbert Irving Comprehensive Cancer Center. This research was funded in part through NIH/NCI Cancer Center Support Grants P30CA013696 to Columbia University, Herbert Irving Comprehensive Cancer Center and P30CA016056 to Roswell Park Comprehensive Cancer Center. The Oncology Precision Therapeutics and Imaging Core (OPTIC) at Columbia and the Comparative Oncology and Flow and Immune Analysis Shared Resources at Roswell Park were utilized in this research. We thank **Santosh Patnaik, MD, PhD**, Assistant Professor at Roswell

Park Comprehensive Cancer Center, for valuable suggestions on experiment design and data analysis.

References:

1. Y. Deng, A. Park, L. Zhu, W. Xie, C. Q. Pan, Effect of semaglutide and liraglutide in individuals with obesity or overweight without diabetes: a systematic review. *Therapeutic Advances in Chronic Disease* **13**, 20406223221108064 (2022).
2. J. Wang, C. H. Kim, Differential Risk of Cancer Associated with Glucagon-like Peptide-1 Receptor Agonists: Analysis of Real-world Databases. *Endocrine Research* **47**, 18-25 (2022).
3. K. Lee, S. Kang, J. Hwang, Lung Cancer Patients' Characteristics and Comorbidities Using the Korean National Hospital Discharge In-depth Injury Survey Data. *Journal of Epidemiology and Global Health* **12**, 258-266 (2022).
4. A. Gupta *et al.*, Premorbid body mass index and mortality in patients with lung cancer: A systematic review and meta-analysis. *Lung Cancer* **102**, 49-59 (2016).
5. N. Shen, P. Fu, B. Cui, C. Y. Bu, J. W. Bi, Associations between body mass index and the risk of mortality from lung cancer: A dose-response PRISMA-compliant meta-analysis of prospective cohort studies. *Medicine (Baltimore)* **96**, e7721 (2017).
6. A. Piening *et al.*, Obesity-related T cell dysfunction impairs immunosurveillance and increases cancer risk. *Nature Communications* **15**, 2835 (2024).
7. J. E. Bader *et al.*, Obesity induces PD-1 on macrophages to suppress anti-tumour immunity. *Nature* **630**, 968-975 (2024).
8. J. Barbi *et al.*, Visceral Obesity Promotes Lung Cancer Progression-Toward Resolution of the Obesity Paradox in Lung Cancer. *J Thorac Oncol* **16**, 1333-1348 (2021).
9. R. J. Smith, Jr. *et al.*, Obesity-specific improvement of lung cancer outcomes and immunotherapy efficacy with metformin. *JNCI: Journal of the National Cancer Institute*, (2024).
10. L. Zhao *et al.*, The key role of a glucagon-like peptide-1 receptor agonist in body fat redistribution. *J Endocrinol* **240**, 271-286 (2019).
11. Y. Zhao *et al.*, The Regulatory Network of CREB3L1 and Its Roles in Physiological and Pathological Conditions. *Int J Med Sci* **21**, 123-136 (2024).

12. C. O'Connor *et al.*, Nfix expression critically modulates early B lymphopoiesis and myelopoiesis. *PLoS One* **10**, e0120102 (2015).
13. A. Ishikawa *et al.*, Loss of Annexin A10 Expression Is Associated with Poor Prognosis in Early Gastric Cancer. *ACTA HISTOCHEMICA ET CYTOCHEMICA* **53**, 113-119 (2020).
14. T. Li *et al.*, Higd1a Protects Cells from Lipotoxicity under High-Fat Exposure. *Oxid Med Cell Longev* **2019**, 6051262 (2019).
15. Q. Zou, H. Qi, Deletion of ribosomal paralogs Rpl39 and Rpl39l compromises cell proliferation via protein synthesis and mitochondrial activity. *Int J Biochem Cell Biol* **139**, 106070 (2021).
16. J. Chen *et al.*, GLP-1 receptor agonist as a modulator of innate immunity. *Front Immunol* **13**, 997578 (2022).
17. M. Ben Nasr *et al.*, Glucagon-like peptide 1 receptor is a T cell-negative costimulatory molecule. *Cell Metab* **36**, 1302-1319.e1312 (2024).
18. C. Zhu *et al.*, Comprehensively prognostic and immunological analyses of GLP-1 signaling-related genes in pan-cancer and validation in colorectal cancer. *Front Pharmacol* **15**, 1387243 (2024).
19. I. Stanisavljevic *et al.*, Semaglutide decelerates the growth and progression of breast cancer by enhancing the acquired antitumor immunity. *Biomed Pharmacother* **181**, 117668 (2024).
20. A. K. O. Rode *et al.*, Induced Human Regulatory T Cells Express the Glucagon-like Peptide-1 Receptor. *Cells* **11**, (2022).
21. I. Hadjiyanni, K. A. Siminovitch, J. S. Danska, D. J. Drucker, Glucagon-like peptide-1 receptor signalling selectively regulates murine lymphocyte proliferation and maintenance of peripheral regulatory T cells. *Diabetologia* **53**, 730-740 (2010).
22. G. M. Delgoffe *et al.*, Stability and function of regulatory T cells is maintained by a neuropilin-1-semaphorin-4a axis. *Nature* **501**, 252-256 (2013).
23. H. Zeng, H. Chi, mTOR signaling in the differentiation and function of regulatory and effector T cells. *Curr Opin Immunol* **46**, 103-111 (2017).
24. A. E. Overacre-Delgoffe *et al.*, Interferon-γ Drives T(reg) Fragility to Promote Anti-tumor Immunity. *Cell* **169**, 1130-1141.e1111 (2017).
25. A. G. Dykema *et al.*, Lung tumor-infiltrating T(reg) have divergent transcriptional profiles and function linked to checkpoint blockade response. *Sci Immunol* **8**, eadg1487 (2023).
26. B. Baban *et al.*, IDO activates regulatory T cells and blocks their conversion into Th17-like T cells. *J Immunol* **183**, 2475-2483 (2009).
27. R. B. Holmgaard *et al.*, Tumor-Expressed IDO Recruits and Activates MDSCs in a Treg-Dependent Manner. *Cell Rep* **13**, 412-424 (2015).
28. E. Mahase, GLP-1 agonists: US sees 700% increase over four years in number of patients without diabetes starting treatment. *Bmj* **386**, q1645 (2024).
29. Y. Xie, T. Choi, Z. Al-Aly, Mapping the effectiveness and risks of GLP-1 receptor agonists. *Nature Medicine*, (2025).
30. J. Zhao *et al.*, Racial difference in BMI and lung cancer diagnosis: analysis of the National Lung Screening Trial. *BMC Cancer* **22**, 797 (2022).
31. J. A. Koehler, T. Kain, D. J. Drucker, Glucagon-like peptide-1 receptor activation inhibits growth and augments apoptosis in murine CT26 colon cancer cells. *Endocrinology* **152**, 3362-3372 (2011).
32. Z. Pu *et al.*, The Effect of Liraglutide on Lung Cancer and Its Potential Protective Effect on High Glucose-Induced Lung Senescence and Oxidative Damage. *FBL* **28**, (2023).
33. H.-j. Zhao *et al.*, Activation of GLP-1 receptor enhances the chemosensitivity of pancreatic cancer cells. *Journal of Molecular Endocrinology* **64**, 103-113 (2020).
34. H. Zhao *et al.*, Activation of glucagon-like peptide-1 receptor inhibits tumourigenicity and metastasis of human pancreatic cancer cells via PI3K/Akt pathway. *Diabetes Obes Metab* **16**, 850-860 (2014).

35. Z. Ungvari *et al.*, Prognostic impact of glucagon-like peptide-1 receptor (GLP1R) expression on cancer survival and its implications for GLP-1R agonist therapy: an integrative analysis across multiple tumor types. *Geroscience*, (2025).
36. A. G. Pachimatla, K. Gee, H. H. Hsiao, S. Yendamuri, S. Rosario, Image-Based Measures of Obesity are Associated with Alterations in Metabolic Pathways in Non-small Cell Lung Cancer. *Ann Surg Oncol*, (2024).
37. M. Ben Nasr *et al.*, Glucagon-like peptide 1 receptor is a T cell-negative costimulatory molecule. *Cell Metab* **36**, 1302-1319 e1312 (2024).
38. S. H. Alharbi, Anti-inflammatory role of glucagon-like peptide 1 receptor agonists and its clinical implications. *Ther Adv Endocrinol Metab* **15**, 20420188231222367 (2024).
39. E. M. da Silva, V. Y. Yariwake, R. W. Alves, D. R. de Araujo, V. Andrade-Oliveira, Crosstalk between incretin hormones, Th17 and Treg cells in inflammatory diseases. *Peptides* **155**, 170834 (2022).
40. X. Lu *et al.*, Liraglutide activates nature killer cell-mediated antitumor responses by inhibiting IL-6/STAT3 signaling in hepatocellular carcinoma. *Transl Oncol* **14**, 100872 (2021).
41. D. Chen, H. Liang, L. Huang, H. Zhou, Z. Wang, Liraglutide enhances the effect of checkpoint blockade through the inhibition of neutrophil extracellular traps in murine lung and liver cancers. *FEBS Open Bio* **n/a**.
42. D. Chen *et al.*, Exenatide enhanced the antitumor efficacy on PD-1 blockade by the attenuation of neutrophil extracellular traps. *Biochem Biophys Res Commun* **619**, 97-103 (2022).
43. Z. Wang *et al.*, Paradoxical effects of obesity on T cell function during tumor progression and PD-1 checkpoint blockade. *Nat Med* **25**, 141-151 (2019).
44. E. V. Mastrolonardo *et al.*, Improved survival with elevated BMI following immune checkpoint inhibition across various solid tumor cancer types. *Cancer* **131**, e35799 (2025).
45. S. Stapleton, G. Welch, L. DiBerardo, L. R. Freeman, Sex differences in a mouse model of diet-induced obesity: the role of the gut microbiome. *Biology of Sex Differences* **15**, 5 (2024).
46. J. Oraha, R. F. Enriquez, H. Herzog, N. J. Lee, Sex-specific changes in metabolism during the transition from chow to high-fat diet feeding are abolished in response to dieting in C57BL/6J mice. *International Journal of Obesity* **46**, 1749-1758 (2022).
47. S. Nishikawa, A. Yasoshima, K. Doi, H. Nakayama, K. Uetsuka, Involvement of sex, strain and age factors in high fat diet-induced obesity in C57BL/6J and BALB/cA mice. *Exp Anim* **56**, 263-272 (2007).
48. B. Fitzgerald *et al.*, A mouse model for the study of anti-tumor T cell responses in Kras-driven lung adenocarcinoma. *Cell Rep Methods* **1**, (2021).
49. B. Langmead, Aligning short sequencing reads with Bowtie. *Curr Protoc Bioinformatics* **Chapter 11**, Unit 11.17 (2010).
50. S. Ghosh, C. K. Chan, Analysis of RNA-Seq Data Using TopHat and Cufflinks. *Methods Mol Biol* **1374**, 339-361 (2016).
51. Y. Liao, G. K. Smyth, W. Shi, The Subread aligner: fast, accurate and scalable read mapping by seed-and-vote. *Nucleic Acids Res* **41**, e108 (2013).
52. M. I. Love, W. Huber, S. Anders, Moderated estimation of fold change and dispersion for RNA-seq data with DESeq2. *Genome Biology* **15**, 550 (2014).
53. J. Reimand *et al.*, Pathway enrichment analysis and visualization of omics data using g:Profiler, GSEA, Cytoscape and EnrichmentMap. *Nat Protoc* **14**, 482-517 (2019).
54. A. Liberzon *et al.*, Molecular signatures database (MSigDB) 3.0. *Bioinformatics* **27**, 1739-1740 (2011).
55. E. L. Jackson *et al.*, The differential effects of mutant p53 alleles on advanced murine lung cancer. *Cancer Res* **65**, 10280-10288 (2005).
56. M. DuPage, A. L. Dooley, T. Jacks, Conditional mouse lung cancer models using adenoviral or lentiviral delivery of Cre recombinase. *Nat Protoc* **4**, 1064-1072 (2009).

57. M. M. Winslow *et al.*, Suppression of lung adenocarcinoma progression by Nkx2-1. *Nature* **473**, 101-104 (2011).
58. E. L. Jackson *et al.*, Analysis of lung tumor initiation and progression using conditional expression of oncogenic K-ras. *Genes Dev* **15**, 3243-3248 (2001).
59. T. Tammela *et al.*, A Wnt-producing niche drives proliferative potential and progression in lung adenocarcinoma. *Nature* **545**, 355-359 (2017).
60. Y. Zhang *et al.*, Activity-balanced GLP-1/GDF15 dual agonist reduces body weight and metabolic disorder in mice and non-human primates. *Cell Metab* **35**, 287-298.e284 (2023).
61. E. Meylan *et al.*, Requirement for NF-kappaB signalling in a mouse model of lung adenocarcinoma. *Nature* **462**, 104-107 (2009).

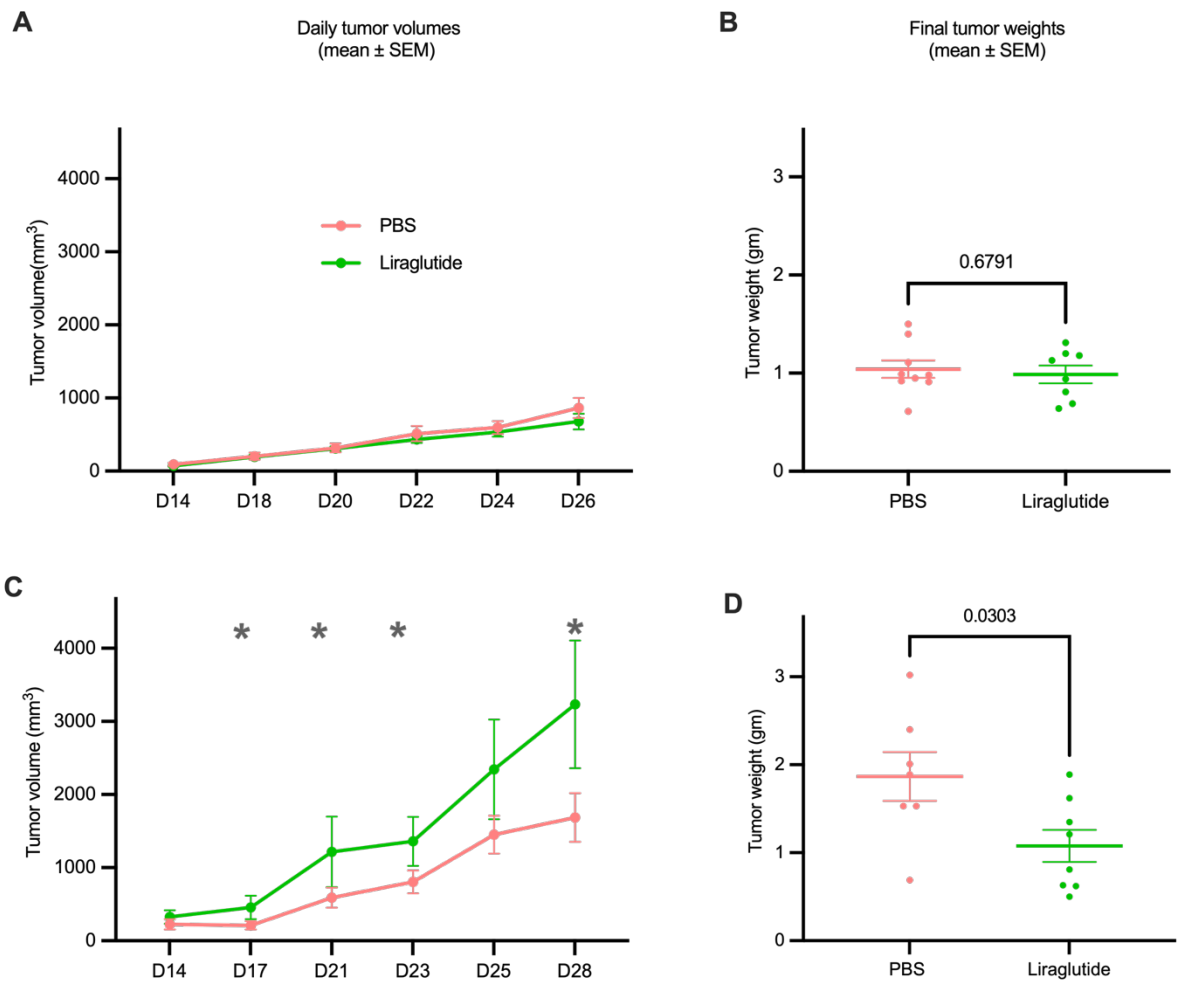

Figure 1. Liraglutide suppresses tumor growth in mice with diet-induced obesity. 7.5x10^4 cells of the KPN1.1 cell lines were injected subcutaneously in the flanks of normal-weight (n=8/group) or obese (n=8/group) C57BL/6 mice fed a control or high-fat diet for 12 weeks, respectively. Once tumors were palpable, mice received daily intraperitoneal injections of Liraglutide or a PBS vehicle. The volumes and weights of tumors in normal-weight mice were not significantly different (A, B). Tumors induced in obese mice had significantly higher volume and end weight in control mice than in liraglutide-treated mice (C, D). Shown are representative findings from at least two independent experiments (n=8 mice/group/trial). SEM = Standard error of mean; PBS = Phosphate buffered saline

*<p=0.05, results of unpaired t-test

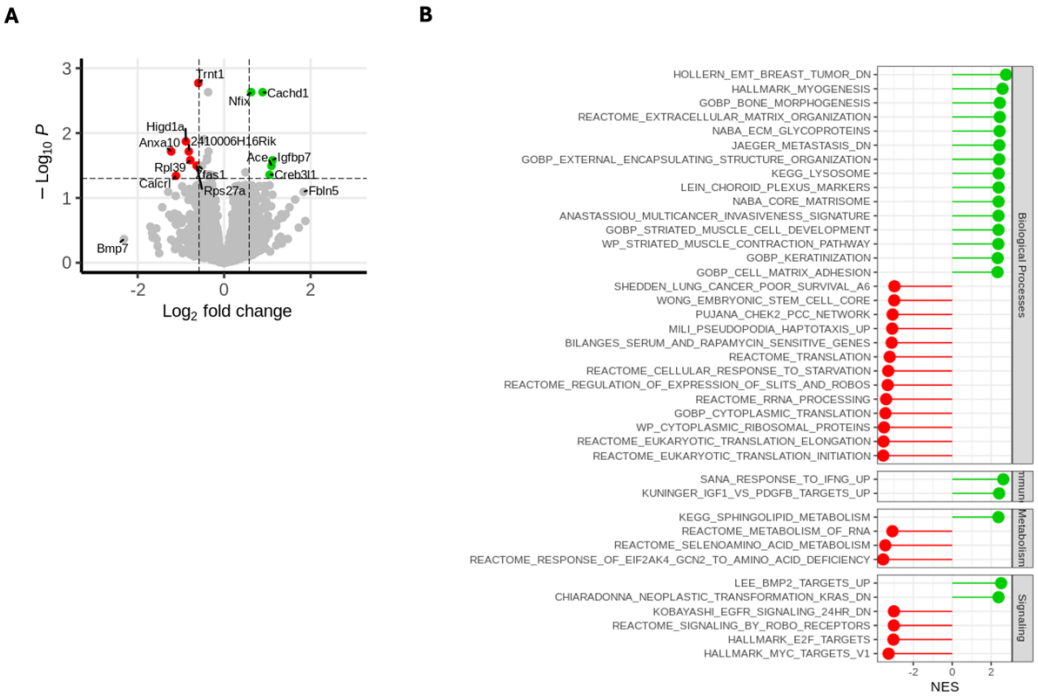

Figure 2. Gene expression changes in tumor cells from obese mice and altered pathways with liraglutide treatment. A) Volcano plot: Differentially expressed genes in liraglutide-treated (green) vs vehicle-treated tumors (red). X-axis: Log2 fold change; Y-axis: Statistical significance. B) Changes in biological processes, immune, cell signaling, and metabolic pathways, as seen by alterations in gene sets, expressed as normalized enrichment score (NES).

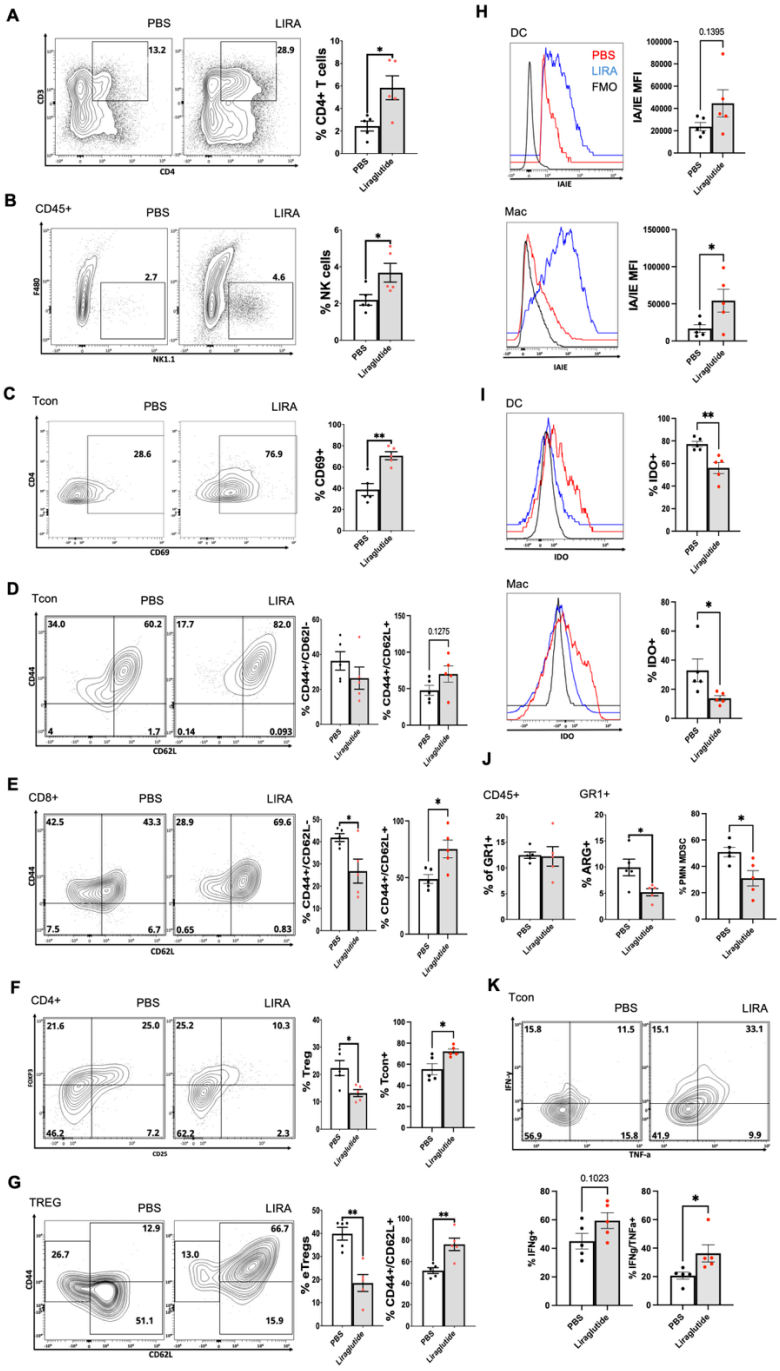

Figure 3. Characterizing the impact of GLP-1Ra treatment on tumor-infiltrating leukocyte populations and phenotypes. Tumor tissues were recovered from the obese mice described in Fig. 2, and, after enzymatic digestion, single-cell suspensions were generated. Immunostaining followed by spectral flow cytometry analysis revealed the effects of LIRA on T cell (panels A-G) and myeloid cell (panels H-J) populations. Flow analysis was also performed to assess intracellular cytokine production by leukocytes re-stimulated ex vivo with PMA/Ionomycin and brefeldin A (K). Shown are the mean +/-SEM results from one of two independent experiments and representative flow plots (n=5 per group/trial). *p < 0.05, **<0.02, ***<0.01, ****<0.001 by t test.

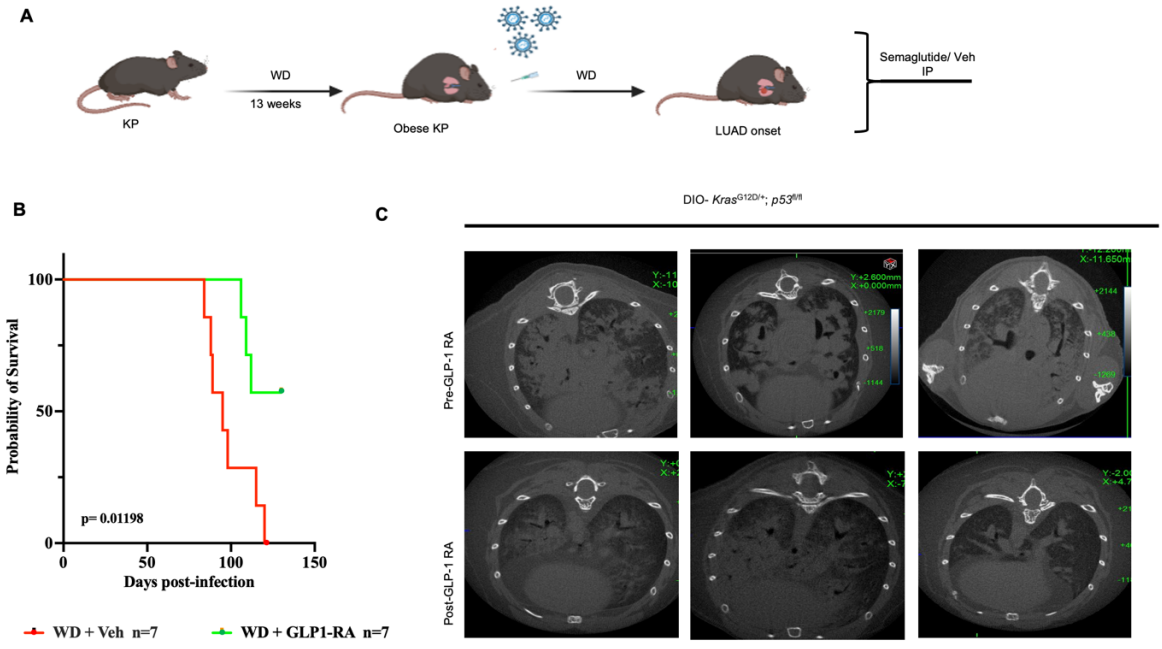

Figure 4. Semaglutide effect in an autochthonous mouse model. A) Schematic illustrating the experimental design in the diet-induced obesity (DIO) KP mouse. B) Kaplan–Meier survival analysis of DIO-KP mice receiving vehicle or semaglutide following tumor initiation (n = 7 per group). Log-rank test (Veh vs Sem): *, P = 0.0119. C) Representative µCT images of lung tumor burden in DIO-KP mice at endpoint, comparing semaglutide- and vehicle-treated groups.

Variable	RFS (Unmatched, n=1177)		RFS (Matched, n=629)		OS (Unmatched, n=1177)		OS (Matched, n=629)	
	Univariable HR (95% CI)	p-value	Univariable HR (95% CI)	p-value	Univariable HR (95% CI)	p-value	Univariable HR (95% CI)	p-value
Age	0.99 (0.98-1.01)	0.45	0.99 (0.97-1.02)	0.39	1.03 (1.01-1.04)	<0.001	1.03 (1.01-1.05)	<0.001
Sex (Female vs. male)	0.70 (0.51-0.96)	0.01	0.82 (0.56-1.19)	0.15	0.65 (0.52-0.81)	0.001	0.56 (0.41-0.77)	0.002
Race (Non-white vs. White)	0.64 (0.33-1.24)	0.09	0.71 (0.34-1.48)	0.18	0.68 (0.43-1.06)	0.045	0.82 (0.48-1.40)	0.24
Smoking (Smoker vs. Non-smoker)	2.53 (0.93-6.87)	0.03	5.59 (0.77-40.49)	0.04	1.53 (0.87-2.69)	0.07	1.16 (0.58-2.30)	0.33
Stage (2 vs. 1)	2.08 (1.49-2.88)	<0.001	2.012 (1.38-2.93)	0.001	1.72 (1.34-2.20)	<0.001	1.54 (1.06-2.23)	0.01
Histology								
Squamous vs Adeno	1.17 (0.82-1.65)	0.18	0.90 (0.53-1.52)	0.35	1.42 (1.15-1.88)	0.001	1.13 (0.78-1.65)	0.25
Other vs Adeno	1.24 (0.77-2.00)	0.18	1.18 (0.62-2.52)	0.30	1.35 (0.95-1.92)	0.043	1.11 (0.67-1.84)	0.09
GLP-1 RA use	0.41 (0.17-1.02)	0.027	0.414 (0.16-1.04)	**0.026**	0.70 (0.43-1.16)	0.09	0.78 (0.44-1.38)	**0.2**

Table 1. Overall survival (OS) and recurrence-free survival (RFS) analyses for overweight and non-overweight NSCLC patients who underwent resection. Univariate analyses were performed using the cox proportional hazards model before and after propensity score matching for age, sex, race, smoking status, stage, histology, and history of GLP-1 RA use (users vs. non-users).

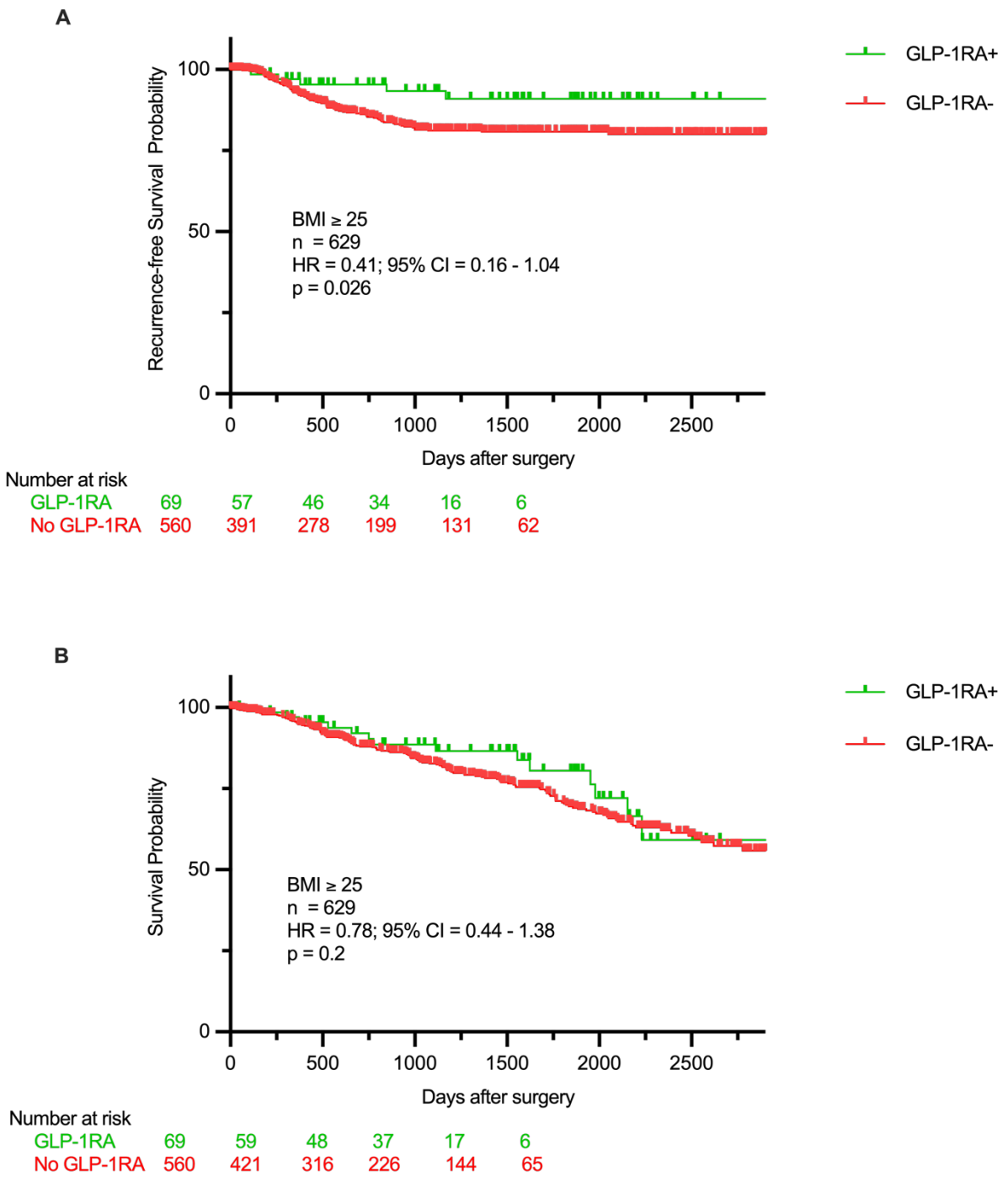

Figure 5. Clinical outcomes with adjuvant GLP-1 RA use after resection in NSCLC. Recurrence-free survival (A) and overall survival (B) in overweight and obese patients who underwent resection for NSCLC and received GLP-1 RA. GLP-1RA use is associated with improved RFS after propensity score matching for age, sex, race, smoking, histology, stage, and GLP-1 RA use as covariates.

Variable	PFS (Unmatched, n=300)		PFS (Matched, n=89)		OS (Unmatched, n=300)		OS (Matched, n=89)	
	Univariable HR (95% CI)	p-value	Univariable HR (95% CI)	p-value	Univariable HR (95% CI)	p-value	Univariable HR (95% CI)	p-value
Age	0.98 (0.97-1.005)	0.09	0.99 (0.95-1.03)	0.38	1.01 (0.99-1.03)	0.03	0.98 (0.94-1.03)	0.29
Sex (Female vs. male)	0.67 (0.34-1.33)	0.13	0.67 (0.34-1.33)	0.13	0.55 (0.41-0.73)	<0.001	0.63 (0.34-1.14)	0.06
Race (Non-white vs White)	1.02 (0.58-1.80)	0.46	1.02 (0.58-1.80)	0.47	2.25 (1.19-4.27)	0.006	3.17 (1.29-7.78)	0.01
Smoking status								
Current vs Never	0.70 (0.37-1.35)	0.14	0.72 (0.23-2.26)	0.28	0.96 (0.51-1.77)	0.45	1.57 (0.22-10.92)	0.32
Former vs Never	0.65 (0.34-1.23)	0.10	0.72 (0.25-2.03)	0.27	0.92 (0.50-1.70)	0.40	1.72 (0.27-10.89)	0.28
Stage (metastatic vs. not)	0.67 (0.37-1.20)	0.09	0.67 (0.37-1.20)	0.09	0.85 (0.60-1.21)	0.19	0.83 (0.54-1.28)	0.42
First-line therapy (Chemo-immunotherapy vs. immunotherapy)	0.94 (0.70-1.26)	0.35	1.08 (0.73-1.61)	0.34	0.89 (0.67-1.18)	0.21	1.22 (0.81-1.83)	0.16
Histology								
Squamous vs adeno	1.09 (0.78-1.52)	0.30	0.96 (0.47-1.94)	0.45	1.61 (1.17-2.21)	0.0015	1.78 (1.009-3.16)	0.02
Other vs adeno	1.20 (0.80-1.71)	0.18	1.64 (1.07-2.50)	0.01	0.91 (0.58-1.42)	0.35	0.72 (0.201-2.61)	0.31
GLP-1 RA use	0.39 (0.13-1.14)	0.044	0.31 (0.1-0.94)	**0.02**	0.40 (0.15-1.04)	0.031	0.41 (0.16-1.01)	**0.027**

Table 2. Overall survival (OS) and progression-free survival (PFS) analyses for overweight and non-overweight NSCLC patients on immune checkpoint inhibitors. Univariate analyses were performed using the Cox proportional hazards model before and after propensity score matching for age, sex, race, smoking status, stage, histology, first-line therapy, and history of GLP-1 RA use (users vs. non-users).

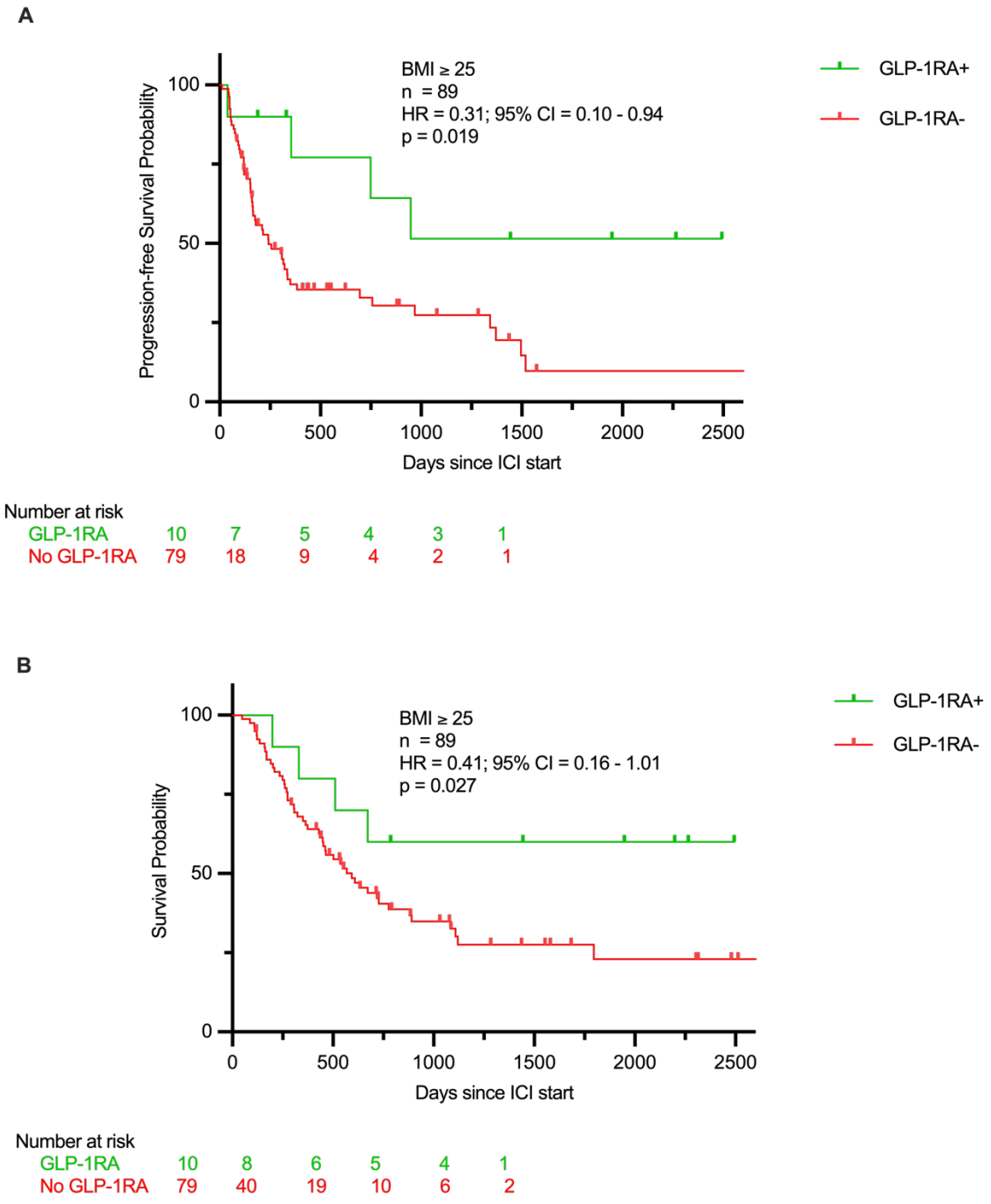

Figure 6. Outcomes with GLP-1 RA use in advanced-stage NSCLC patients on ICI. Progression-free survival (A) and overall survival (B) in overweight and obese patients receiving ICI for advanced NSCLC after propensity score matching for age, sex, race, smoking, histology, stage, first-line therapy, and GLP-1RA use as covariates.